PROCEEDINGS OF SCIENCE

Single and double Dalitz decays of π^0, η and η' through rational approximants

Sergi Gonzàlez-solís[*†]
Institut de Física d'Altes Energies (IFAE), The Barcelona Institute of Science and Technology, Campus Universitat Autònoma de Barcelona, 08193 Bellaterra (Barcelona)
E-mail: sgonzalez@ifae.cat

We analyze the single and double Dalitz decays $\mathscr{P} \to \ell^+\ell^-\gamma$ and $\mathscr{P} \to \ell^+\ell^-\ell^+\ell^-$ ($\mathscr{P} = \pi^0, \eta, \eta'$; $\ell = e$ or μ), by means of a data-driven approach based on the use of rational approximants applied to π^0, η and η' transition form factor experimental data collected in the space-like energy region. Predictions for the mass spectra and branching ratios are given and compared with current experimental status.

The 8th International Workshop on Chiral Dynamics
29 June 2015 - 03 July 2015
Pisa, Italy

[*]Speaker.
[†]I would like to thank the organizers for the nice and interesting workshop we have enjoyed.

PoS(CD15)126

1. Introduction

A single(double) Dalitz decay proceeds through the reaction $\mathscr{P} \to \gamma^*\gamma^{(*)}$ ($\mathscr{P} = \pi^0, \eta, \eta'$) after the conversion of the virtual photon(s) into a lepton pair(s). Since $\mathscr{P}$ has an internal structure a transition form factor (TFF) comes into play encoding the QCD dynamics effects occurring in the $\mathscr{P}\gamma^*\gamma^{(*)}$ vertex. The singly virtual TFF, which depends on the transferred momentum to the virtual photon, can be parameterized by means of Vector Meson Dominance (VMD) after the (dispersive) spectral representation in q^2 (with q^2 the photon virtuality)

$$F_{\mathscr{P}\gamma\gamma^*}(q^2) = \int_{s_0}^{\infty} ds \frac{\rho(s)}{s - q^2 - i\varepsilon}\,, \tag{1.1}$$

with s_0 the threshold for physical intermediate states and when the contribution to the spectral function of a single narrow-width resonance reduces to $\rho(s) \propto \pi\delta(s - M_{\text{eff}}^2)$, which yields

$$F_{\mathscr{P}\gamma\gamma^*}(q^2) = \frac{F_{\mathscr{P}\gamma\gamma}(0)}{1 - \frac{q^2}{\Lambda^2}}\,, \tag{1.2}$$

where $\Lambda(= M_{\text{eff}}^2)$ accounts for the position of the pole on the real q^2 axis. However, this description breaks down for $q^2 = \Lambda^2$, corresponding to an on-shell intermediate resonance. A common way to cure this limitation is by incorporating width effects into the propagator, $\Gamma(q^2)$, whose standard form for more than one single particle contribution reads [1]

$$F_{\mathscr{P}\gamma\gamma^*}(q^2) = F_{\mathscr{P}\gamma\gamma}(0) \left(\sum_{V=\rho,\omega,\phi} \frac{g_{\mathscr{P}V\gamma}}{2g_{V\gamma}} \right)^{-1} \sum_{V=\rho,\omega,\phi} \frac{g_{\mathscr{P}V\gamma}}{2g_{V\gamma}} \frac{M_V^2}{M_V^2 - q^2 - iM_V\Gamma_V(q^2)}\,, \tag{1.3}$$

where $g_{\mathscr{P}V\gamma}$ and $g_{V\gamma}$ are, respectively, the $\mathscr{P}V\gamma$ and $V\gamma$ couplings while the expression for the width reads $\Gamma_V(q^2) = \Gamma_V \frac{q^2}{M_V^2} \frac{\sigma^3(q^2)}{\sigma^3(M_V^2)}$ with $\sigma(s)$ a kinematical factor i.e. $\sigma(q^2) = \sqrt{1 - 4M_\pi^2/q^2}$ for $V = \rho$. For our study, we benefit from the works of refs. [2, 3], where the current experimental data of the modulus of the space-like TFF $\gamma^*\gamma \to \mathscr{P}$ [5] have successfully been accommodated in a simple way through the use of Padé approximants [6], to represent the modulus of the time-like partner transition $\mathscr{P} \to \gamma^*\gamma$. Our main goal is to predict the spectra and the branching ratio of the single and double Dalitz decays we are interested in. Other different parameterizations existing in the literature are based on resonance chiral theory [7, 8] and on dispersive techniques [9, 10], among others [11, 12, 13, 14, 15, 16, 17, 18].

In this talk we address the following topics: in section 2, our description of the modulus transition form factor in the time-like energy region is discussed and compared with current experimental determinations. In sections 3 and 4 we tackle the main features of the single and double Dalitz decays under evaluation. Section 5 is devoted to the conclusions including our central branching ratio predictions.

2. Transition form factor

Padé approximants (PA) are meromorphic functions, in our case ratios of a polynomial of order N and a polynomial of order M, constructed in such a manner that their Taylor expansion

coincide with that of the (unknown) function to be approximated up to order $\mathscr{O}(q^2)^{M+N+1}$

$$P_M^N(q^2) = \frac{\sum_{i=0}^{N} a_i (q^2)^i}{\sum_{j=0}^{M} b_j (q^2)^j}\,. \tag{2.1}$$

We argue that eq. (1.2) can be seen as the $P_1^0(Q^2)$ PA to the TFF that is, the first element of the general sequence given by eq. (2.1). Despite the fact that the convergence of the sequence to the function we want to approximate is only ensured for a special kind a functions (*e.g.* functions of Stieltjes type and/or meromorphic) a pattern may be inferred from data. For instance, the excellent performance of PAs in ref. [2, 3, 4, 19] seems to indicate that the convergence is ensured at the energies we are exploring. On the other hand, one cannot extend the TFF as parameterized for describing the space-like energy regime to reproduce the entire TFF in the time-like since this region may contain isolated poles and branch cuts. Strictly speaking, there is no *a priori* reason why PAs should work above the branch cut developed at the $\pi\pi$ threshold. We argue that the imaginary part of the $\pi\pi$ at threshold is subleading [19] and, therefore, the absolute value of the TFF is well approximated by a real meromorphic function which has nothing but isolated poles. In this scenario, PAs are an excellent approximation tool. In our description, PAs can be used as long as $\lim_{N\to\infty} f(q^2) - P_M^N(q^2) = 0 \in \mathscr{D}$ is satisfied provided that the energy domain $\mathscr{D}$ does not contain any pole. For the case that concerns us, PAs represent the modulus of the TFF of the $\mathscr{P}\gamma^*\gamma$ vertex after fitting the corresponding experimental data in the space-like region. The transition $\pi^0 \to \gamma^*\gamma$ occurs at very low-momentum transfer and can be expressed by the Taylor expansion of eq. (2.1)

$$F_{\pi^0\gamma^*\gamma}(q^2) = F_{\pi^0\gamma^*\gamma}(0)\left(1 + b_\pi \frac{q^2}{m_\pi^2} + c_\pi \frac{q^4}{m_\pi^4} + \mathscr{O}(q^6)\right), \tag{2.2}$$

with $F_{\pi^0\gamma\gamma}(0)$ fixed from the experimental width to two photons while the values of the low energy parameters, slope (b_π) and curvature (c_π), are borrowed from the analysis of ref. [2]. For the η, in fig. 1 (up panel) we provide a graphical account of the modulus of the TFF (normalized to unity at the origin) in the time-like energy regime after extrapolating the parameterization of the space-like fits as obtained in ref. [3]. The comparison with the current experimental determinations from $\eta \to e^+e^-\gamma$ (black circles) and $\eta \to \mu^+\mu^-\gamma$ (green squares) obtained, respectively, by the A2 and NA60 collaborations [20] is shown in nice agreement. The description of the TFF of the η' through PAs is more delicate since, in this case, the pole lies within the available phase space (see right panel of table 4 of ref. [3]) and, hence, we cannot describe the whole transition by the use of PAs. We, then, proceed to match the prediction as given by PA to eq. (1.3) by letting the coupling $g_{\rho\gamma}$ to float, whose value will precisely be inferred when performing the matching. Therefore, the representation below the matching point is given by the PA while above by eq. (1.3) with the corresponding value for the $g_{\rho\gamma}$ coupling. We have chosen the values of the rest of the required couplings from table 4 of ref. [4] and then we have performed the matching point at the latest experimental data point fixed at 0.75 GeV (see ref. [22] for further details). This exercise is graphically represented in fig. 1 (down panel) and compared, with very good agreement, with the current data reported by BESIII collaboration [21]. Regarding the TFF of double virtuality, which depends on both photon virtualities, is commonly described by the factorization approach $F_{\mathscr{P}\gamma^*\gamma^*}(q_1^2, q_2^2) = F_{\mathscr{P}\gamma^*\gamma}(q_1^2, 0) F_{\mathscr{P}\gamma\gamma^*}(0, q_2^2)$, where the right-hand functions are given by the singly virtual TFF we have already described. However, this ansatz, though reasonable since we lack

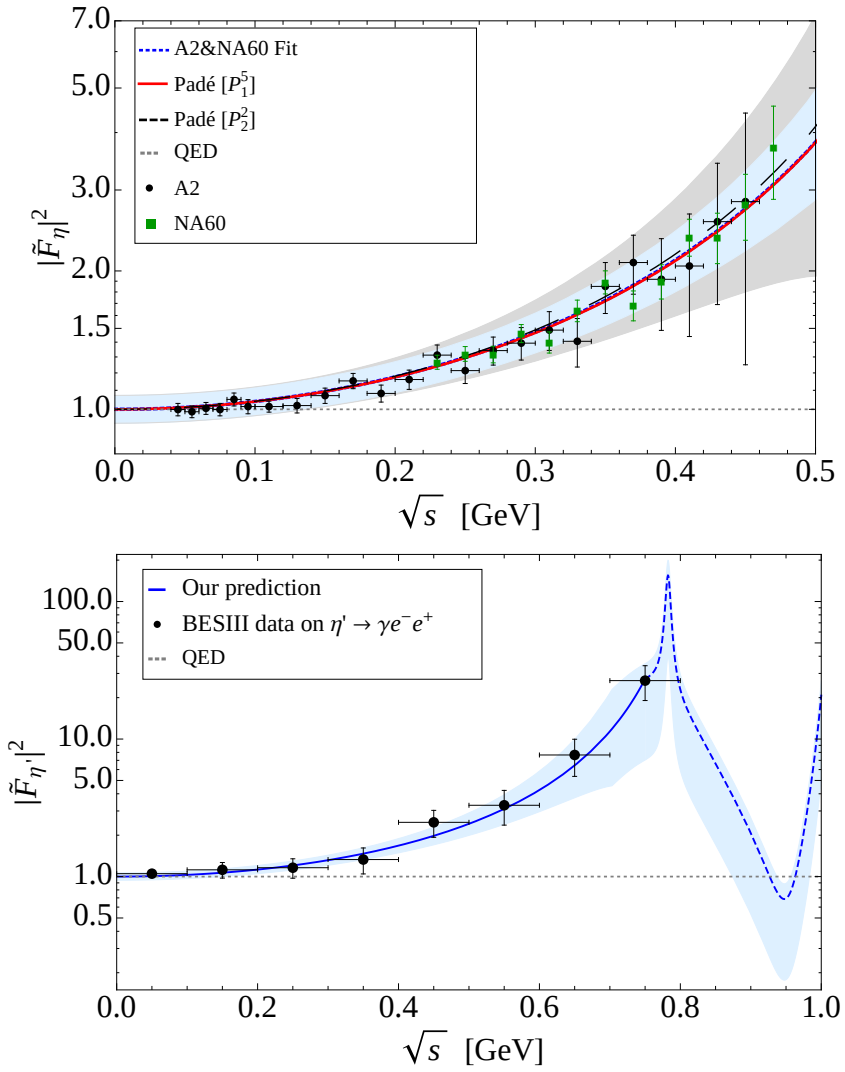

Figure 1: up: Representation of the modulus squared of the TFF (normalized to unity at the origin) of the η meson in the time-like as given by the PAs $P_1^5(\sqrt{s})$ and $P_2^2(\sqrt{s})$ (red solid and black dashed curves respectively) together with the one sigma error band (light-blue and light gray respectively). **down:** Time-like description of the η' TFF as given by $P_1^6(\sqrt{s})$ for the region below the matching point at 0.75 GeV (blue solid curve) and by eq. (1.3) above (blue dashed curve). The error bands include also the uncertainty associated of the partial decay width to two photons

experimental information in this case, induce a q^{-4} term violating the OPE limit which tell us $\lim_{q^2\to\infty} F(q_1^2, q_2^2) \sim q^{-2}$ [23]. We can cure this fact by reconstructing the doubly virtual TFF through the use of the so-called Chisholm approximants (CA) [6, 24] (see also refs. [25, 26]), a bivariate generalization of the PAs, whose lowest order bivariate reads

$$P_1^0(q_1^2, q_2^2) = \frac{a_{0,0}}{1 + \frac{b_{1,0}}{M_{\mathscr{P}}^2}(q_1^2 + q_2^2) + \frac{b_{1,1}}{M_{\mathscr{P}}^4} q_1^2 q_2^2}, \tag{2.3}$$

where $a_{0,0}$ is fixed from the experimental decay width to two photon to the value of the TFF at the origin of energies, $b_{1,0}$ is the slope of the singly virtual TFF obtained in refs. [2, 3], while $b_{1,1}$ would

correspond to the doubly virtual slope which for our predictions we vary, as a conservative estimate, from $b_{1,0} = 0$ respecting the OPE to $b_{1,2} = 2b_{1,0}^2$, far from the factorization result $b_{1,1}^2 = b_{1,0}^2$. For our final predictions (preliminary) we have considered both the standard factorization approach as well as the CA in a combined weighted average way. See also ref. [27] for a recent description of the TFF of double virtuality of the η meson.

3. Single and double Dalitz decays

R. Dalitz postulated in 1951 the decay $\pi^0 \to e^+e^-\gamma$ [28]. The energy release in the process is small and the TFF effects are tiny as can be seen in fig. 2 (left panel) where we display the decay distribution as function of the e^+e^- invariant mass as compared to the pure QED calculation (see ref. [29] for QED radiative corrections on this process). The decay is mainly dominated by the very low-energy region of the spectrum where the effect of TFF is negligible. A similar pattern is followed by the single Dalitz decays $\eta \to e^+e^-\gamma$ and $\eta' \to e^+e^-\gamma$. On the contrary, when muons come up in the final state, the effects of the TFF appear to be much notorious since the decay width is more homogeneously distributed. Double Dalitz decays follow basically the same trend. Here we can differentiate between two scenarios depending whether the final state dilepton pairs are equal. As a matter of example, in figs. 2 and 3 we provide the decay distribution for $\eta \to e^+e^-e^+e^-$ as a function of one di-electron invariant mass of the direct diagram (right panel in fig. 2) as well as the distribution of the decay $\eta' \to e^+e^-\mu^+\mu^-$ (down panel in fig. 3) as a function of the angle ϕ formed between the planes of the two di-lepton pairs (described in the upper panel of fig. 3). In the full electronic decay of the η we show, in particular, the contribution from the direct diagram (green solid curve), the curve of the exchange diagram expressed in terms of the former di-electron invariant mass of the direct diagram (red dotted curve), the interference term (which is destructive and represented by the blue dotted curve) and the total decay rate distribution (black dotted line) whereas from the $e^+e^-\mu^+\mu^-$ mode of the η' we learn that the decay is most probable when the two planes are perpendicular (*i.e.* when $\phi = \pi/2$).

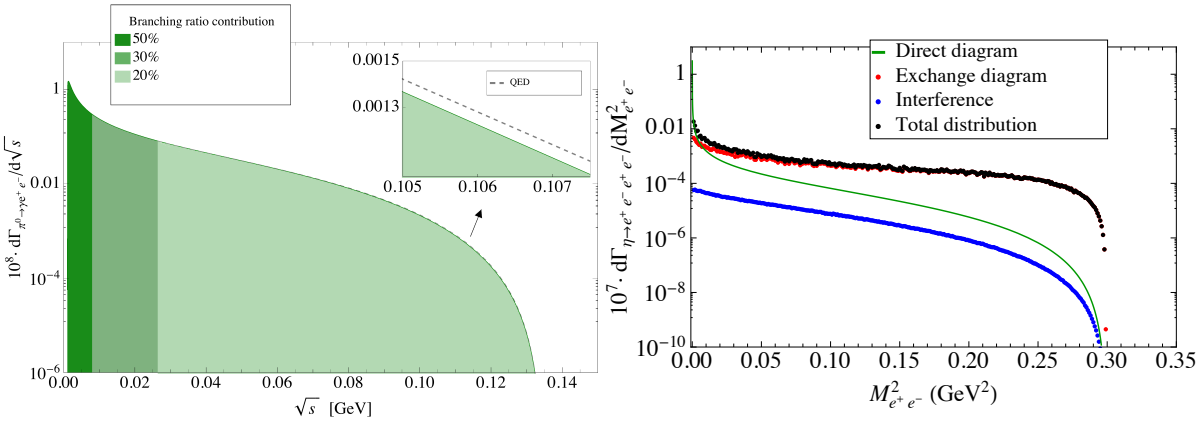

Figure 2: Decay distribution for $\pi^0 \to e^+e^-\gamma$ (left) and for $\eta \to e^+e^-e^+e^-$ (right) as a function of the e^+e^- invariant mass. The exchange diagram and the interference term as expressed in the figure of the right have required a Monte Carlo integration.

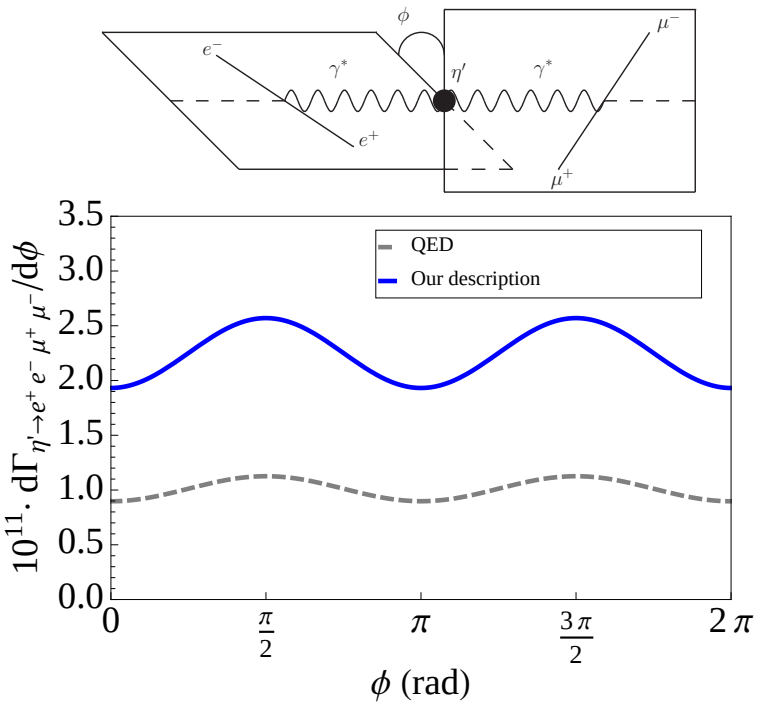

Figure 3: Decay distribution for $\eta' \to e^+e^-\mu^+\mu^-$ (down) shown as a function of the angle ϕ formed by the planes of the two di-lepton pairs (up).

4. Conclusions

We predict the single and double Dalitz decays $\mathscr{P} \to \ell^+\ell^-\gamma$ and $\mathscr{P} \to \ell^+\ell^-\ell^+\ell^-$ ($\mathscr{P} = \pi^0, \eta, \eta'$; $\ell = e$ or μ) benefited from a data-driven description of the modulus of the transition form factor $\mathscr{P} \to \gamma^*\gamma^{(*)}$ which is nicely supported by current experimental data as displayed in fig. 1. We have seen that the modulus of the TFF is well approximated by a meromorphic function in terms of rational approximants. From the phenomenological point of view, the processes involving electrons in the final state are less sensitive to the TFF than when muons come into play because the decay distribution of the former is vastly dominated by the region of low momentum transfer. Furthermore, TFF effects are enhanced for η' decays because of phase space considerations. Our (preliminary) central branching ratio predictions are displayed and compared with current experimental status in table 1 (we have shown previous results in ref. [30]). I would like to further encourage experimental hadron facilities to measure those still unknown observables and see whether they corroborate our predictions.

Decay	This work	Measurement
$\pi^0 \to e^+e^-\gamma$	$1.169(33)\%$	$1.174(35)\%$
$\eta \to e^+e^-\gamma$	$6.61(59)\cdot 10^{-3}$	$6.90(40)\cdot 10^{-3}$
$\eta \to \mu^+\mu^-\gamma$	$3.27(56)\cdot 10^{-4}$	$3.1(4)\cdot 10^{-4}$
$\eta' \to e^+e^-\gamma$	$4.38(24)\cdot 10^{-4}$	$4.69(20)(23)\cdot 10^{-4}$
$\eta' \to \mu^+\mu^-\gamma$	$0.75(7)\cdot 10^{-4}$	$1.08(27)\cdot 10^{-4}$
$\pi^0 \to e^+e^-e^+e^-$	$3.37(9)\cdot 10^{-5}$	$3.34(16)\cdot 10^{-5}$
$\eta \to e^+e^-e^+e^-$	$2.71(2)\cdot 10^{-5}$	$2.4(2)(1)\cdot 10^{-5}$
$\eta \to \mu^+\mu^-\mu^+\mu^-$	$3.98(15)\cdot 10^{-9}$	$< 3.6\cdot 10^{-4}$
$\eta \to e^+e^-\mu^+\mu^-$	$2.38(7)\cdot 10^{-6}$	$< 1.6\cdot 10^{-4}$
$\eta' \to e^+e^-e^+e^-$	$2.11(50)\cdot 10^{-6}$	unobserved
$\eta' \to \mu^+\mu^-\mu^+\mu^-$	$1.68(47)\cdot 10^{-8}$	unobserved
$\eta' \to e^+e^-\mu^+\mu^-$	$6.36(1.07)\cdot 10^{-7}$	unobserved

Table 1: Our (preliminar) central branching ratio predictions.

Acknowledgments

I would like to thank Rafel Escribano, Pere Masjuan and Pablo Sanchez-Puertas for discussions and the referee of the manuscript for comments on the analytical structure of our description. This work was supported in part by the FPI scholarship BES-2012-055371, the Ministerio de Ciencia e Innovación under grant FPA2011-25948, the Ministerio de Economía y Competitividad under grants CICYT-FEDER-FPA 2014-55613-P and SEV-2012-0234, the Secretaria d'Universitats i Recerca del Departament d'Economia i Coneixement de la Generalitat de Catalunya under grant 2014 SGR 1450, and the Spanish Consolider-Ingenio 2010 Programme CPAN (CSD2007-00042).

References

[1] L. G. Landsberg, Phys. Rept. **128**, 301 (1985).

[2] P. Masjuan, Phys. Rev. D **86**, 094021 (2012) [arXiv:1206.2549 [hep-ph]].

[3] R. Escribano, P. Masjuan and P. Sanchez-Puertas, Phys. Rev. D **89**, 034014 (2014) [arXiv:1307.2061 [hep-ph]].

[4] R. Escribano, P. Masjuan and P. Sanchez-Puertas, Eur. Phys. J. C **75**, no. 9, 414 (2015) [arXiv:1504.07742 [hep-ph]].

[5] H. J. Behrend *et al.* [CELLO Collaboration], Z. Phys. C **49**, 401 (1991); J. Gronberg *et al.* [CLEO Collaboration], Phys. Rev. D **57**, 33 (1998) [hep-ex/9707031]; B. Aubert *et al.* [BaBar Collaboration], Phys. Rev. D **80**, 052002 (2009) [arXiv:0905.4778 [hep-ex]]; P. del Amo Sanchez *et al.* [BaBar Collaboration], Phys. Rev. D **84**, 052001 (2011) [arXiv:1101.1142 [hep-ex]]; S. Uehara *et al.* [Belle Collaboration], Phys. Rev. D **86**, 092007 (2012) [arXiv:1205.3249 [hep-ex]]; M. Acciarri *et al.* [L3 Collaboration], Phys. Lett. B **418**, 399 (1998).

[6] G. A. Baker and P. Graves-Morris, Encyclopedia of Mathematics and Its Applications (Cambridge University Press, Cambridge, England, 1996).

[7] H. Czyz, S. Ivashyn, A. Korchin and O. Shekhovtsova, Phys. Rev. D **85**, 094010 (2012) [arXiv:1202.1171 [hep-ph]].

[8] P. Roig, A. Guevara and G. López Castro, Phys. Rev. D **89**, no. 7, 073016 (2014) [arXiv:1401.4099 [hep-ph]].

[9] C. Hanhart, A. Kupść, U.-G. Meißner, F. Stollenwerk and A. Wirzba, Eur. Phys. J. C **73**, no. 12, 2668 (2013) [arXiv:1307.5654 [hep-ph]].

[10] M. Hoferichter, B. Kubis, S. Leupold, F. Niecknig and S. P. Schneider, Eur. Phys. J. C **74**, 3180 (2014) [arXiv:1410.4691 [hep-ph]].

[11] C. -C. Lih, J. Phys. G **38**, 065001 (2011) [arXiv:0912.2147 [hep-ph]].

[12] C. Q. Geng and C. C. Lih, Phys. Rev. C **86** (2012) 038201 [Phys. Rev. C **87** (2013) 3, 039901] [arXiv:1209.0174 [hep-ph]].

[13] I. Balakireva, W. Lucha and D. Melikhov, Phys. Rev. D **85**, 036006 (2012) [arXiv:1110.6904 [hep-ph]].

[14] Y. Klopot, A. Oganesian and O. Teryaev, Phys. Rev. D **87**, no. 3, 036013 (2013) [Phys. Rev. D **88**, no. 5, 059902 (2013)] [arXiv:1211.0874 [hep-ph]]; Y. Klopot, A. Oganesian and O. Teryaev, JETP Lett. **99**, 679 (2014) [arXiv:1312.1226 [hep-ph]].

[15] S. S. Agaev, V. M. Braun, N. Offen, F. A. Porkert and A. SchÂŁfer, Phys. Rev. D **90**, no. 7, 074019 (2014) [arXiv:1409.4311 [hep-ph]].

[16] J. Bijnens and F. Perrsson, hep-ph/0106130.

[17] T. Petri, arXiv:1010.2378 [nucl-th].

[18] C. Terschlüsen, B. Strandberg, S. Leupold and F. Eichstädt, Eur. Phys. J. A **49**, 116 (2013) [arXiv:1305.1181 [hep-ph]].

[19] R. Escribano, S. Gonzàlez-Solís, P. Masjuan and P. Sanchez-Puertas, arXiv:1512.07520 [hep-ph].

[20] R. Arnaldi *et al.* [NA60 Collaboration], Phys. Lett. B **677**, 260 (2009) [arXiv:0902.2547 [hep-ph]]; P. Aguar-Bartolome *et al.* [A2 Collaboration], Phys. Rev. C **89**, 044608 (2014) [arXiv:1309.5648 [hep-ex]].

[21] M. Ablikim *et al.* [BESIII Collaboration], Phys. Rev. D **92**, no. 1, 012001 (2015) [arXiv:1504.06016 [hep-ex]].

[22] R. Escribano and S. Gonzàlez-Solís, arXiv:1511.04916 [hep-ph].

[23] H. Suura, T. F. Walsh and B. L. Young, Lett. Nuovo Cim. **4S2**, 505 (1972) [Lett. Nuovo Cim. **4**, 505 (1972)]; G. Kopp, T. F. Walsh and P. M. Zerwas, Nucl. Phys. B **70**, 461 (1974); K. S. Babu and E. Ma, Phys. Lett. B **119**, 449 (1982); V. A. Novikov, M. A. Shifman, A. I. Vainshtein, M. B. Voloshin and V. I. Zakharov, Nucl. Phys. B **237** (1984) 525.

[24] P. Masjuan and P. Sanchez-Puertas, arXiv:1504.07001 [hep-ph].

[25] P. Sanchez-Puertas and P. Masjuan, arXiv:1510.06564 [hep-ph].

[26] P. Sanchez-Puertas and P. Masjuan, arXiv:1510.05607 [hep-ph].

[27] C. W. Xiao, T. Dato, C. Hanhart, B. Kubis, U.-G. Meißner and A. Wirzba, arXiv:1509.02194 [hep-ph].

[28] R. H. Dalitz, Proc. Phys. Soc. A **64**, 667 (1951).

[29] T. Husek, K. Kampf and J. Novotný, Phys. Rev. D **92**, no. 5, 054027 (2015) [arXiv:1504.06178 [hep-ph]].

[30] S. Gonzàlez-Solís, Nucl. Part. Phys. Proc. **258-259**, 94 (2015). P. Adlarson *et al.*, arXiv:1412.5451 [nucl-ex].